γ-Tubulin Is Essential for Acentrosomal Microtubule Nucleation and Coordination of Late Mitotic Events in *Arabidopsis* [W]

Pavla Binarová,[a,1,2] Věra Cenklová,[b,1] Jiřina Procházková,[a,c,1] Anna Doskočilová,[a] Jindřich Volc,[a] Martin Vrlík,[a] and László Bögre[c]

[a] Institute of Microbiology, Academy of Sciences of the Czech Republic, 142 20 Prague 4, Czech Republic
[b] Institute of Experimental Botany, Academy of Sciences of the Czech Republic, 772 00 Olomouc, Czech Republic
[c] School of Biological Sciences, Royal Holloway, University of London, Egham TW20 OEX, United Kingdom

γ-Tubulin is required for microtubule (MT) nucleation at MT organizing centers such as centrosomes or spindle pole bodies, but little is known about its noncentrosomal functions. We conditionally downregulated γ-tubulin by inducible expression of RNA interference (RNAi) constructs in *Arabidopsis thaliana*. Almost complete RNAi depletion of γ-tubulin led to the absence of MTs and was lethal at the cotyledon stage. After induction of RNAi expression, γ-tubulin was gradually depleted from both cytoplasmic and microsomal fractions. In RNAi plants with partial loss of γ-tubulin, MT recovery after drug-induced depolymerization was impaired. Similarly, immunodepletion of γ-tubulin from *Arabidopsis* extracts severely compromised in vitro polymerization of MTs. Reduction of γ-tubulin protein levels led to randomization and bundling of cortical MTs. This finding indicates that MT-bound γ-tubulin is part of a cortical template guiding the microtubular network and is essential for MT nucleation. Furthermore, we found that cells with decreased levels of γ-tubulin could progress through mitosis, but cytokinesis was strongly affected. Stepwise diminution of γ-tubulin allowed us to reveal roles for MT nucleation in plant development, such as organization of cell files, anisotropic and polar tip growth, and stomatal patterning. Some of these functions of γ-tubulin might be independent of MT nucleation.

INTRODUCTION

Plants possess a highly dynamic microtubular cytoskeleton in which several arrays, such as the interphase cortical microtubules (MTs), perinuclear prophase MTs, mitotic spindle, and phragmoplast, are temporally separated during the cell cycle. Higher plant cells lack a defined centrosome, and all of these MT arrays are nucleated from flexible dispersed sites of unknown composition.

γ-Tubulin is a highly conserved protein in eukaryotes that was found to be localized to centrosomes and other defined microtubule organizing centers (MTOCs). The MTOC-associated γ-tubulin provides a minus end nucleation template for MT growth (Moritz et al., 1995). However, MTs are nucleated even in the absence of MTOC-associated γ-tubulin. Centrosomal γ-tubulin was depleted by RNA interference (RNAi) in *Caenorhabditis elegans* and *Drosophila* cell lines, but some unknown mechanism still supported the partial assembly of mitotic asters

and the formation of abnormal spindles (Strome et al., 2001; Hannak et al., 2002; Raynaud-Messina et al., 2004). γ-Tubulin participates in pathways for MT nucleation that are independent of centrosome or spindle pole bodies even in the cell where these MTOCs are present (Vorobjev et al., 2001; Venkatram et al., 2005). Molecular mechanisms underlying the function of noncentrosomal γ-tubulin are poorly understood.

In the Bryophyta, MTs are organized on poles and γ-tubulin localization changes from these polar organizers to mitotic microtubular arrays (Brown et al., 2004). In higher plants, γ-tubulin was first immunolocalized in the vicinity of nuclei and in association with all of the microtubular arrays. Based on immunolocalization studies of γ-tubulin, the nuclear envelope was considered a site for plant MT nucleation from which MTs are transported to the cell cortex (Liu et al., 1993; Vaughn and Harper, 1998; Schmit, 2002). However, green fluorescent protein–tubulin labeling showed constant treadmilling of MTs on the cortex, whereas transport of preformed MTs from the nuclear region to the cortex has never been observed (Shaw et al., 2003). Complementation of a γ-tubulin mutation in *Schizosaccharomyces pombe* was the first functional study strongly suggesting a conserved role for plant γ-tubulin in MT nucleation (Horio and Oakley, 2003). Our previous studies showed that the majority of plant γ-tubulin was present with membranes in the form of protein complexes, whereas a smaller portion of γ-tubulin was associated with plant MTs in vivo and in vitro. We proposed that the flexibility of MT nucleation is ensured by the association of γ-tubulin–dependent nucleation sites with dynamic membranes and MTs (Drykova

et al., 2003). There is a growing body of evidence that such extracentrosomal MT nucleation elements travel on MTs in polarized epithelial cells (Reilein and Nelson, 2005) and in cells of *S. pombe* (Janson et al., 2005) or can nucleate MTs from membranes (Chabin-Brion et al., 2001). MT-dependent nucleation of cortical MTs by γ-tubulin was recently described in tobacco (*Nicotiana tabacum*) cells (Murata et al., 2005). The emerging resemblance of extracentrosomal MT organizing templates in mammalian cells, fungi, and plants might reflect conserved mechanisms for noncentrosomal MT nucleation.

Besides the relatively well-characterized roles for γ-tubulin in MT nucleation, there are other functions that might be unrelated to MT nucleation in animals and fungi. In *S. pombe* and *Aspergillus nidulans*, conditional mutants in γ-tubulin were defective in mitotic spindle checkpoints, leading to aberrant cytokinesis (Hendrickson et al., 2001; Prigozhina et al., 2004). γ-Tubulin mutants in *S. pombe* have defects in the regulation of MT length, suggesting a role in MT stability (Paluh et al., 2000). In *Aspergillus*, γ-tubulin was proposed to regulate cell cycle progression independent of its function as a MT nucleator (Prigozhina et al., 2004). γ-Tubulin was also found in nuclear complexes that link DNA recombination with centrosomal function (Lesca et al., 2005). The characteristics of plant γ-tubulin, such as its relatively high abundance compared with animal cells or fungi and its presence in various cell compartments, including nuclei, are also suggestive of multiple and perhaps divergent roles (Binarova et al., 2000).

Here, we address the in vivo role for γ-tubulin using inducible RNAi techniques to downregulate γ-tubulin transcript levels in *Arabidopsis thaliana*. We show that γ-tubulin is essential for noncentrosomal MT nucleation in plants. Induced diminution of γ-tubulin revealed the functional importance of dynamic γ-tubulin redistributions during cell division. Moreover, reduced γ-tubulin levels disrupted processes that are associated with the specification of cell identity, such as stomatal patterning. Our studies provide new insights into multiple cellular and developmental functions for γ-tubulin in acentrosomal cells.

RESULTS

Generation of Plant Lines with Downregulated γ-Tubulin Levels by RNAi

There are two γ-tubulin genes in *Arabidopsis* with 94% similarity at the DNA level. To downregulate both γ-tubulin genes, we prepared an RNAi construct with an inverted repeat corresponding to the 722-bp fragment of the 3′ terminal part of *Arabidopsis* TubG1 mRNA and placed it under the control of a dexamethasone-inducible promoter. The expression cassette was designed to incorporate the reporter gene, β-glucuronidase (GUS), under the control of the same dexamethasone-inducible promoter to detect the level of induction. We stably transformed this construct into the *Arabidopsis* activator line 4C-S5 (Craft et al., 2005) and obtained 40 independent transformants. These were screened for phenotypic changes induced by 20 μM dexamethasone that cosegregated 3:1 with hygromycin resistance and GUS expression in the T2 generation. The T-DNA insert was further verified by PCR in these lines. T2 generation seedlings from 10 chosen

lines having a single T-DNA insert were germinated in the presence or absence of 20 μM dexamethasone and screened for phenotypic responses. On average, 60% of seedlings within these lines responded to dexamethasone induction of RNAi expression by phenotypic changes of different strengths (see below).

We also prepared an RNAi construct with the same inverted repeat of γ-tubulin sequence under the control of an ethanol-inducible promoter (Deveaux et al., 2003). The BASTA-resistant T2 generation was screened for phenotypic responses to RNAi induction by exposing seedlings to 0.2% ethanol on agar plates or watering in soil as described previously (Ketelaar et al., 2004). We obtained seven lines in which 60% of seedlings showed phenotypic changes after ethanol induction of RNAi expression.

A range of common phenotypic changes occurred equally at the plant and cellular levels with both of the inducible expression systems, strongly suggesting a link to γ-tubulin downregulation upon RNAi expression. Based on the severity of the induced abnormalities in the individual dexamethasone- and ethanol-inducible γ-tubulin RNAi lines, we established categories of strong, mild, and weak phenotypes. Approximately 5% of plants exhibited a strong phenotype after RNAi induction; seedlings germinated on dexamethasone-containing medium had thick and short primary roots and died at the cotyledon stage (Figures 1A and 1B). Malformed seedlings with frequent calli-like protrusions could not recover when transferred to medium without dexamethasone. Fragile seedlings indicated a defect in cell wall formation. This strong phenotype was rarely observed (~1% of seedlings) also with the ethanol-inducible system. The second group of transformants, displaying a mild phenotype, was the most abundant, 60 to 70%. Plants with dexamethasone- and ethanol-induced RNAi expression developed fragile, thick, curled true leaves that often turned pale green. They failed to flower and were dying 2 to 3 weeks after induction. Plants with the mild RNAi phenotype that developed 20 d after dexamethasone induction are shown in Figure 1C as representatives. In the course of this work, we analyzed the cellular and morphological phenotypes with both inducible RNAi lines, concentrating on plants with mild phenotypic effects and gradual γ-tubulin downregulation (see also Figures 3 to 8 below). The third group of transformants, occurring with ~30% frequency with both inducible systems, showed weak phenotypes and flowered under inductive conditions for RNAi expression. However, as demonstrated with plants grown on long-term dexamethasone induction, leaf rosettes were more compact, internode length was reduced, and siliques were short (Figure 1D). In the dexamethasone-inducible system, in most cases the strength of the phenotype correlated with the level of GUS expression upon induction (see Supplemental Figure 1 online). None of these phenotypes was observed in transformants without dexamethasone treatment or in plants transformed with an empty vector grown with or without dexamethasone. In the ethanol-inducible system, we occasionally observed weak root phenotypes without inducer, indicating some leakage in the expression system.

To determine the reduction in γ-tubulin levels upon induction of the RNAi construct, we performed protein gel blot analysis on seedlings taken from several independent lines showing variable strength of the phenotypes. In extracts from pooled seedlings
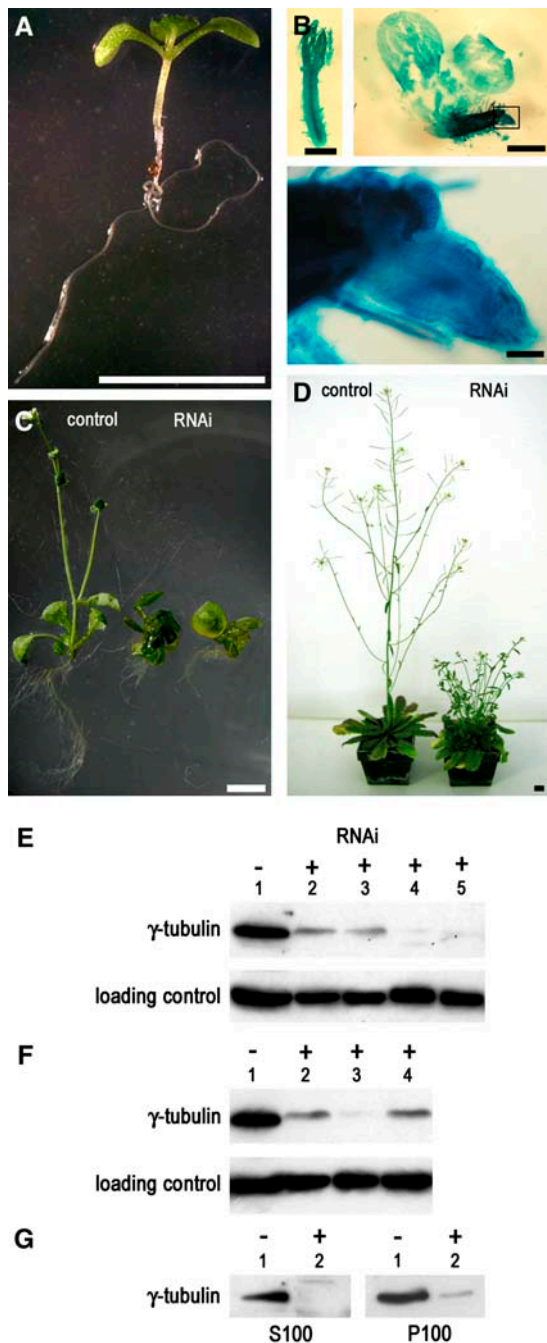
Figure 1. Developmental Abnormalities in *Arabidopsis* Lines with RNAi-Induced Downregulation of γ-Tubulin.

(A) Control uninduced *Arabidopsis* seedling transformed with dexamethasone-inducible RNAi construct 10 d after germination. Bar = 1 cm.

(B) Strong phenotype in a representative dexamethasone-induced RNAi γ-tubulin seedling, 10 d after germination on medium with dexamethasone, showing growth arrest and lethality at the cotyledon stage. Histochemical GUS staining revealed strong inducible expression of the coregulated marker. As shown at left and in the enlarged boxed area, the main root is arrested and new auxiliary meristems are activated. Bars = 1 mm.

(C) Mild RNAi phenotype in two representative dexamethasone-induced

with strong phenotypes (Figure 1B), the γ-tubulin levels were severely reduced 5 d after dexamethasone treatment and were depleted to undetectable levels 10 d after induction (Figure 1E). We determined the γ-tubulin levels in ∼100 individual RNAi plants taken from independent transformed lines of both inducible systems showing mild phenotypes (Figure 1C). A convincing correlation between the gradual reduction of γ-tubulin protein levels and the severity of phenotypes was found in plants with both dexamethasone-inducible (Figure 1F, lanes 2 and 3) and ethanol-inducible (Figure 1F, lane 4) γ-tubulin RNAi constructs.

Previously, we showed that a major portion of plant γ-tubulin is recovered in the microsomal fraction; thus, membrane compartments were suggested to be important for plant acentrosomal MT nucleation (Drykova et al., 2003). Therefore, crude extracts from control plants and from plants that expressed the dexamethasone-inducible RNAi construct were fractionated to cytoplasmic and microsomal fractions, and γ-tubulin levels were found to be proportionally reduced in both (Figure 1G).

Depletion of γ-Tubulin Impairs MT Nucleation

To asses how MTs are affected by RNAi depletion of γ-tubulin, we performed immunofluorescence labeling for α- and γ-tubulin on seedlings in the strong phenotype category 10 d after induction with dexamethasone. The levels of γ-tubulin decreased below detectable levels by immunofluorescence, and MTs were absent from the cells (Figure 2A); this is consistent with the protein gel blot analysis that indicated severe depletion of γ-tubulin (Figure 1E). These cells looked abnormal and had extremely large vacuoles, their nuclei were pushed from the central position to the cell wall, and the cytoplasm was reduced to narrow strands around the nucleus.
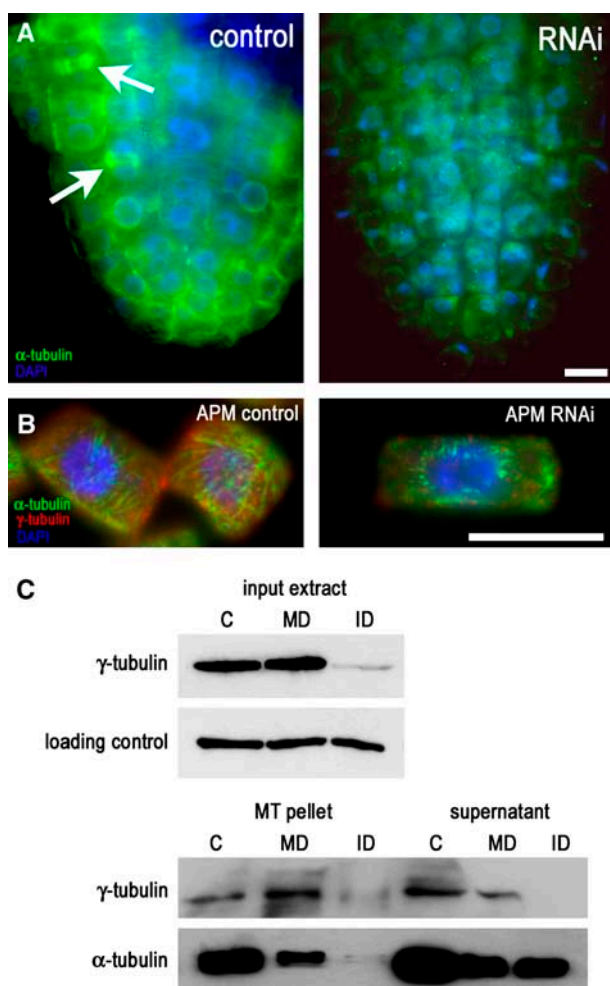
γ-tubulin RNAi seedlings. Shown are a control uninduced plant and two RNAi plants 20 d after induction with arrested development. Bar = 1 cm.

(D) Weak γ-tubulin RNAi phenotype with reduced elongation growth. Control and dexamethasone-induced γ-tubulin RNAi plants were grown in soil for 50 d under continuous dexamethasone treatment. Bar = 1 cm.

(E) Immunoblot analysis of γ-tubulin in total protein extracts from dexamethasone-inducible γ-tubulin RNAi plants with the strong phenotype as shown in **(B)** arrested at the cotyledon stage. Lane 1, uninduced control; lanes 2 and 3, pooled seedlings 5 d after induction; lanes 4 and 5, pooled seedlings 10 d after induction.

(F) γ-Tubulin in seedlings with the mild phenotype as shown in **(C)**. γ-Tubulin was analyzed by immunoblotting in total protein extracts from individual γ-tubulin RNAi plants. Lane 1, uninduced control; lane 2, plants with dexamethasone-induced RNAi for 15 d; lane 3, dexamethasone induction for 20 d; lane 4, plants with ethanol-induced RNAi for 15 d. Samples were loaded at the same protein content (40 μg/lane). Shown are typical examples of protein gel blot analysis selected from ∼100 analyzed RNAi plants, all showing a corresponding reduction in γ-tubulin levels with the severity of the phenotypes.

(G) Distribution of γ-tubulin in cytoplasmic and membrane fractions from RNAi plants 15 d after induction. S100, high-speed supernatant; P100, microsomal pellet. Lane 1, uninduced control; lane 2, induced RNAi plant. To compare the relative distribution of γ-tubulin, pelleted material was resuspended in a volume equal to that of the corresponding supernatant.

The lack of MTs in cells with RNAi-depleted γ-tubulin as well as the accompanying cellular changes indicated that γ-tubulin is essential for the formation of plant MTs. Because of the severe abnormalities in these cells, the loss of MTs could also be a secondary effect. Therefore, we further investigated the nucleation role of γ-tubulin in plants with mild phenotypes in which 10 d of dexamethasone-induced RNAi expression reduced γ-tubulin levels by ~70%. MTs were present in these cells, so we followed their recovery after depolymerization using the drug amiprophos methyl (APM) in dexamethasone-induced and uninduced plants. Figure 2B shows that in uninduced plants, MTs started to regrow from the perinuclear and cortex regions 15 min after the removal of APM. Contrary to this, in cells induced for the expression of the RNAi construct, MT regrowth was much slower, and only a few short, thick bundles of MTs were recovered in the vicinity of nuclei 1 h after APM removal (Figure 2B).

To further confirm the role for γ-tubulin in MT nucleation, we depleted γ-tubulin from cell extracts and performed in vitro polymerization assays from cell extracts of *Arabidopsis*, as described previously (Drykova et al., 2003). γ-Tubulin was almost completely eliminated from the extracts by immunodepletion, whereas in the mock experiment, γ-tubulin protein levels were not significantly changed (Figure 2C). The immunodepleted extracts were used as the input extracts in MT spin-down experiments. Data from spin-down experiments showed that taxol-driven polymerization of MTs from γ-tubulin–immunodepleted extracts was severely impaired, whereas MTs from the control or from the mock-depleted extracts were able to polymerize. The failure of MT polymerization from the extracts immunodepleted for γ-tubulin was also observed microscopically on slides by visualizing MTs with both immunofluorescence and differential interference contrast (DIC) optics (see Supplemental Figure 2 online). Together, the absence of MTs after RNAi depletion or immunodepletion of γ-tubulin and the limited MT recovery in cells with partial reduction of γ-tubulin level suggest that γ-tubulin is essential for MT nucleation and polymerization in vivo in plants and in vitro in cell extracts.

Figure 2. RNAi Depletion and Immunodepletion of γ-Tubulin Impair Plant MT Nucleation.

(A) α-Tubulin labeling in an RNAi plant (strong phenotype as shown in Figure 1B) grown for 10 d on dexamethasone. Mitotic microtubular arrays were immunolabeled in control root tip cells (arrows), whereas in RNAi seedlings, MTs were largely absent and cells had extreme vacuolization and small nuclei close to the cell walls. DAPI, 4′,6-diamidino-2-phenylindole. Bar = 10 μm.
(B) Recovery of MTs after depolymerization by the drug APM. In control uninduced plants, MT regrowth was observed at 15 min after removal of APM. In plants (mild phenotype as shown in Figure 1C) with dexamethasone RNAi expression induced for 10 d, the level of γ-tubulin was partially reduced, and a few short, thick bundles of MTs were recovered in the vicinity of nuclei 1 h after APM removal. Bar = 10 μm.
**(C)** In vitro polymerization of MTs in extracts immunodepleted for γ-tubulin. Taxol-driven polymerization from input extracts is shown in the top panel, followed by immunoblot analysis for α- and γ-tubulin of pelleted MTs and supernatants in the bottom panel. No MTs were pelleted from extracts immunodepleted for γ-tubulin. C, control; ID, immunodepleted; MD, mock-depleted.

Organization of Cortical MTs Is Sensitive to RNAi-Induced Reduction of γ-Tubulin Levels

In *Arabidopsis* uninduced control cells, γ-tubulin is distributed on the cortex and along cortical MTs in a patchy pattern. The cellular distribution of γ-tubulin was altered in cells after RNAi induction; the signal for immunolabeled γ-tubulin rapidly disappeared from cortical MTs in plants of the mild phenotype category 5 d after induction with dexamethasone (Figure 3A). Although almost complete RNAi depletion of γ-tubulin prevents MT polymerization, partial depletion allows MTs to be formed but affects the organization of specific subsets of MTs. The regular transverse arrangement of cortical MTs in roots of *Arabidopsis* plants was randomized 5 d after RNAi induction with dexamethasone, and MTs became shortened and bundled (Figure 3B). This finding was similar in both dexamethasone- and ethanol-inducible systems and indicates that cortical MTs rapidly responded to the reduction in γ-tubulin levels.
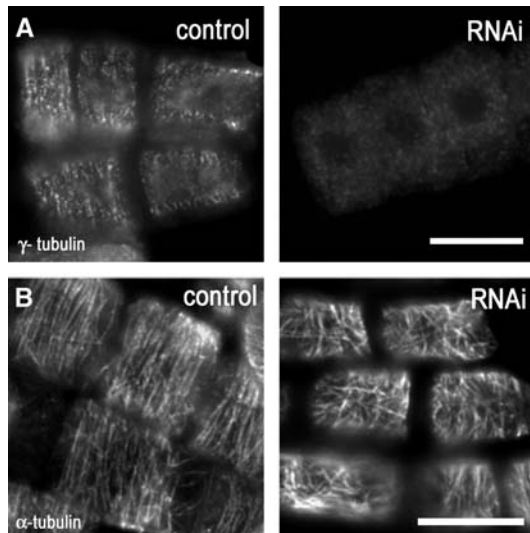
Figure 3. Organization of Cortical MTs Is Sensitive to Decreased γ-Tubulin Levels.

(A) γ-Tubulin and DNA labeling in roots of control and dexamethasone-inducible RNAi plants (mild phenotype). γ-Tubulin was distributed on the cortex and along cortical MTs in a patchy pattern in control plants, and the signal for γ-tubulin rapidly disappeared from cortical MTs in RNAi-expressing plants 5 d after induction with dexamethasone. Bar = 10 μm. **(B)** Parallel arrangements of cortical MTs in control plants became randomized in RNAi plants 5 d after induction with dexamethasone. Bar = 10 μm.

Reduction of γ-Tubulin by RNAi Affects Cytokinesis

Next, we examined how the reduced γ-tubulin levels affect cell division in roots in which division planes are strictly controlled, leading to precisely organized cell files. Although γ-tubulin in higher plant cells is not associated with discrete polar MTOCs such as centrosomes, its punctate staining on mitotic MTs, in the polar region, and in the region of phragmoplast and cell plate formation shows bipolarity from prophase to telophase (Drykova et al., 2003). Here, we show that γ-tubulin is gradually depleted from all of these polar locations in cells with RNAi expression (Figures 4A and 4B). In animal cells, depletion of centrosome-associated γ-tubulin leads to monopolar or multipolar spindles during mitosis (Hannak et al., 2002), but this was rarely observed in our experiments, and despite the reduction of spindle-associated γ-tubulin, spindles remained focused to acentrosomal poles (Figure 4B). In some cases when γ-tubulin was severely depleted, spindles collapsed and only remnants of MTs remained in the vicinity of chromosomes (Figure 4C).

Compared with the precisely organized cell files of the control (Figure 4A), patches of cells with defective arrangements of cell walls were observed in RNAi-expressing plants in both dexamethasone- and ethanol-inducible systems. As shown in Figure 4B for plants grown for 10 d with dexamethasone induction, dividing root cells with reduced levels of γ-tubulin were able to progress through mitosis, but misaligned cell walls and binuclear cells revealed that cytokinesis was severely impaired. Immunofluorescent labeling confirmed that γ-tubulin levels were

significantly reduced in these cells. Misoriented phragmoplasts and cell division planes were the most common cytokinetic defects we observed in cells with reduced γ-tubulin levels (Figures 4B and 4D) and led to distortion of regular cell files, as shown also in Figure 5. We also found phragmoplasts with bundled and disorganized MTs (Figure 4E). In some cells, the early-stage solid phragmoplast persisted between separated nuclei that already showed decondensed chromatin (Figure 4F). Thus, the expansion into a late ring-like phragmoplast and the corresponding cell plate expansion were delayed beyond the nuclear cycle or were absent in cells with reduced levels of γ-tubulin. Prolonged RNAi induction for 20 d led to severe depletion of γ-tubulin and to the absence of MTs; cells frequently became binuclear (Figure 4G).

The cytokinetic abnormalities observed in γ-tubulin RNAi plants suggest that the presence of γ-tubulin on mitotic spindle poles and its timely translocation to the site of cell plate formation during the anaphase-to-telophase transition are important for the spatial and temporal coordination of late mitotic events.

Organization of Cell Files and Anisotropic Cell Expansion in Roots Are Both Affected by RNAi Reduction of γ-Tubulin Levels

To assess the role of γ-tubulin in plant development, we analyzed RNAi plants with gradually reduced γ-tubulin within the mild phenotype category (Figure 1C). In control roots, cells are strictly organized into files radially and into meristematic, elongation, and differentiation zones longitudinally. Radial expansion of cells initially became obvious in the elongation zone of RNAi-expressing seedlings 5 to 6 d after germination on inductive medium with dexamethasone or ethanol. Instead of anisotropic growth, cells became isodiametric, enlarged with small nuclei dislocated close to the cell wall, and some binuclear cells appeared, as shown in dexamethasone-induced RNAi plants 5 d after induction (Figure 5A). With increased RNAi induction in time, even cells in the meristematic zone became highly vacuolated and nuclei became shifted from the central position to the site of cell division, which indicated an arrest in cell cycle progression and a loss of stem cell identity within the meristem (Figure 5B). Observation of root epidermal cells revealed that the cell files were interrupted with clusters of disoriented cells or that the files with regularly elongated cells were interrupted with clusters of aberrant cells in which anisotropic growth was lost (Figure 5C). All cell files became disorganized in roots of RNAi plants grown under dexamethasone- or ethanol-induced conditions; the malformed root of a plant grown for 15 d with dexamethasone is shown in Figure 5D. The aberrant root morphogenesis is consistent with the observation of grossly misaligned phragmoplasts and aberrant cytokinesis (Figure 4). Membrane staining with FM1-43 and propidium iodide staining, which penetrates membranes of damaged cells, revealed the presence of dead cells; clusters of small nuclei stained with propidium iodide were closely packed together without any sign of being organized into cell files. The meristematic cell clusters were interspersed within large, highly vacuolated isodiametric cells with extensive callose deposition. Epidermal cells were extremely enlarged, forming bulges.
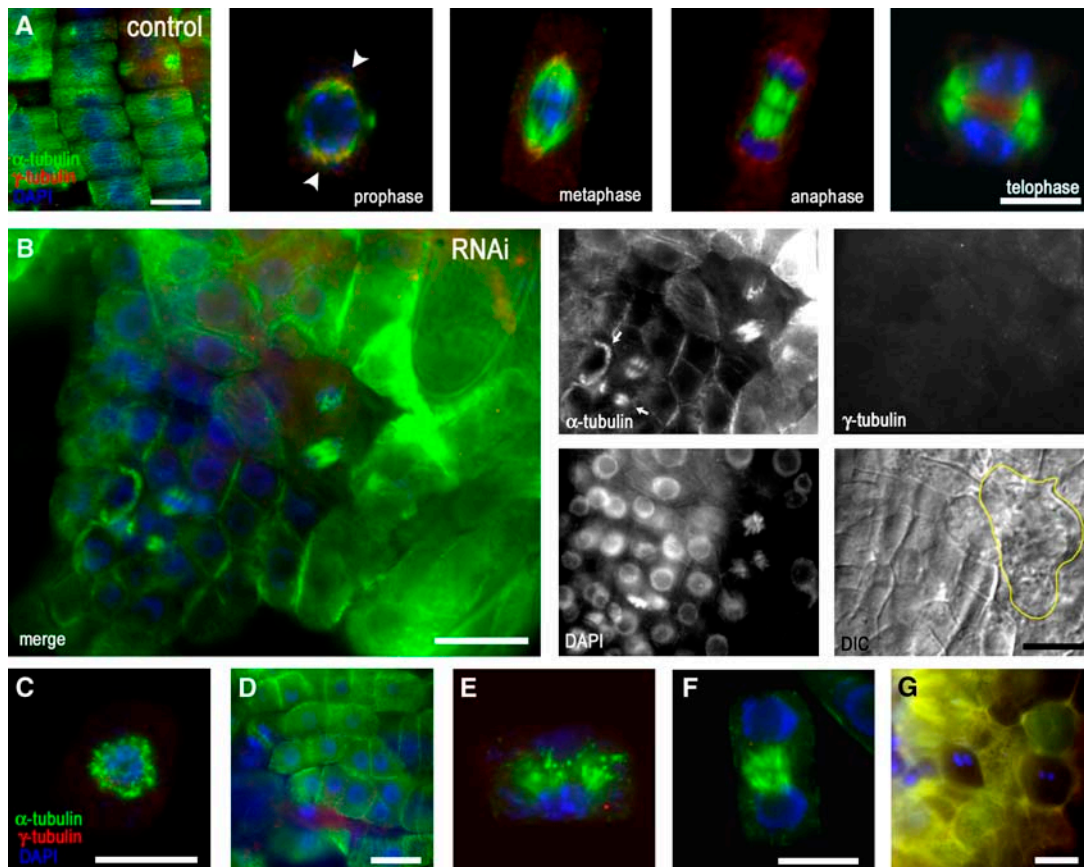
Figure 4. γ-Tubulin RNAi in Dividing Cells of *Arabidopsis* Roots Affect Cytokinesis and the Organization of Cell Files.

(A) Whole-mount α-tubulin (green) and γ-tubulin (red) immunolabeling and DAPI staining of DNA (blue) of control uninduced seedlings having regularly arranged cell files. γ-Tubulin in the root cells of the control exhibits bipolar localization from prophase (arrowheads) to telophase when it accumulates in the phragmoplast and the forming cell plate area.

(B) Whole-mount α-tubulin (green) and γ-tubulin (red) immunolabeling and DAPI staining of DNA (blue) of RNAi-expressing seedlings with mild phenotypes and reduced γ-tubulin levels 10 d after dexamethasone induction. Shown are a merged image (left panel), α-tubulin, γ-tubulin, DAPI staining, and DIC image (four small right panels). MTs are still present in mitotic cells, with spindles focused to acentrosomal poles, but cytokinesis became defective. The phragmoplasts are misaligned (arrows), and the organization of cell files is disrupted. The yellow line indicates the shape of a binuclear cell in the DIC image. Dividing cells are surrounded by enlarged cells with callose deposits.

(C) Collapsed spindle with MTs randomly arranged in the vicinity of chromosomes in a cell with severely depleted γ-tubulin 15 d after induction with dexamethasone.

(D) Misorientation of cell division planes in roots expressing ethanol-induced RNAi for 10 d.

(E) Phragmoplast with bundled and disorganized MTs in roots expressing dexamethasone-induced RNAi for 10 d.

(F) Early solid phragmoplast persists between separated nuclei with already decondensed chromatin, as revealed by DAPI staining. The expanded ring-like phragmoplast is present in this late stage of cytokinesis in the control cells **(A)**.

(G) Cells are often binuclear in seedlings 20 d after induction, with severe depletion of γ-tubulin.

Bars = 10 μm.

γ-Tubulin Is Important for Initiation and Tip Growth of Root Hair Cells

In control uninduced plants, the transition between the elongation zone and the differentiation zone is marked by the exclusive presence of root hairs that develop according to defined positional patterns and elongate by a process known as tip growth. Root hair development was severely disrupted with dexamethasone- and ethanol-inducible γ-tubulin RNAi expression. This is shown on a root 8 d after dexamethasone treatment in which ectopic root hair formation was observed along the entire root length (Figure 6A). Closer inspection revealed that elimination of γ-tubulin affected both pattern formation and morphogenesis of root hairs. The nucleus was misplaced in the bulge, and sometimes two nuclei were present within the same root hair, stacked beneath an extremely large vacuole (Figure 6B). In wild-type plants, root hairs grow in a single axis from an initiated bulge. Root hairs that developed with reduced levels of γ-tubulin often failed to form a single axis, and bulges with two or more growth axes were observed (Figure 6C). In plants with severely depleted γ-tubulin,
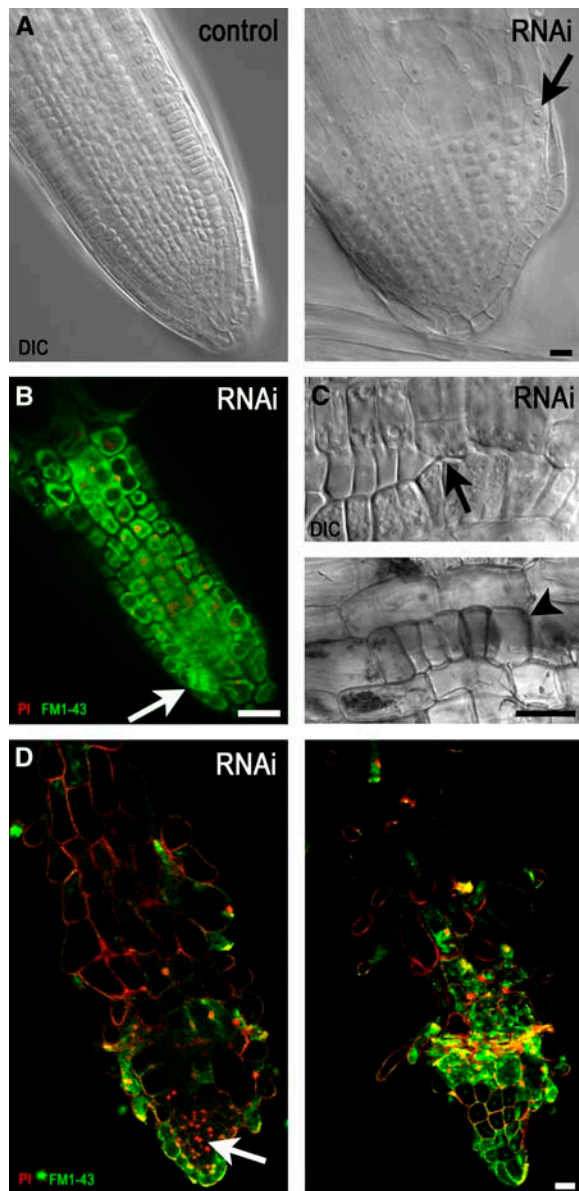
Figure 5. The Organization of Root Cell Files Is Distorted with RNAi-Induced Diminution of γ-Tubulin.

(A) DIC images of a root from an uninduced control plant (left) with cells organized as files and the root of an RNAi plant (right) 5 d after dexamethasone induction with radial expansion and with binuclear cells (arrow).

(B) Confocal laser scanning microscopy single optical section of a root tip of an RNAi plant 10 d after dexamethasone induction. FM1-43 membrane staining and propidium iodide (PI) nuclear staining showed that cells in the meristematic zone became vacuolated, with nuclei shifted from a central position, whereas cell division sites were often misaligned (arrow).

(C) Patches of epidermal cells with misaligned cell walls (top, arrow) or clusters of isodiametric epidermal cells (bottom, arrowhead) in the elongation zone of RNAi plants 10 d after induction of RNAi with ethanol shown in DIC images.

(D) Confocal laser scanning microscopy single optical sections through

the bulge did not develop further, suggesting the failure of transition from the initiation stage to root hair tip growth (Figure 6D). Many independent experiments with both inducible systems showed that the root hair phenotype is frequent in plants expressing RNAi (Figures 6B to 6D), and such abnormalities were not found or were found only rarely in uninduced controls or in plants transformed with empty vector grown with or without dexamethasone or ethanol induction. We quantitated the root hair abnormalities for both inducible systems, but results are shown only for the dexamethasone induction (Figure 6E). Our data demonstrate that the cell fate specification during root hair initiation, the regular transition from root hair initiation to tip growth, and the maintenance of a single growth axis all require a minimal level of γ-tubulin.

Decreased γ-Tubulin Levels Alter Leaf Development and Stomatal Patterning

The observed RNAi phenotype of the aerial parts of plants was similar in both dexamethasone- and ethanol-inducible systems. The aberrant leaf morphology of plants with the mild phenotype (Figure 1C) grown for 15 d with ethanol induction is shown in Figures 7A to 7D. True leaves of RNAi-expressing plants were thick and curled, with extensive adaxial growth and a rough blade surface (Figure 7A). The youngest true leaves that developed under severe depletion of γ-tubulin were several times thicker than control leaves, often with club-shaped blades suggesting a complete loss of dorsoventral polarity (Figure 7B). Trichomes were fewer in number and had extremely swollen bases (Figure 7C), prolonged RNAi induction resulted in un-branched trichomes (Figure 7D), and trichomes were completely absent under severe depletion of γ-tubulin (Figure 7B).

As shown in Figure 1D, transformants with a weak phenotype showed elongation defects, but leaves presented no visible morphological differences. However, closer inspection revealed defects in stomatal patterning. Stomata development follows a strict developmental pattern, a fundamental aspect of which is the so-called one-cell-spacing rule: stomata do not contact each other directly. To maintain the rule, stomata are formed by at least one asymmetric and one symmetric division controlled by position-dependent cell signaling (Geisler et al., 2003). Contrary to the control, clusters of two to four stomata were present in leaves of soil-grown plants in which the expression of the RNAi construct was induced by dexamethasone, although the division of stomata was completed (Figure 8A). Immunofluorescent staining revealed the presence of MTs in guard cells of clustered stomata, apparently without significant changes in arrangement (Figure 8B). In inflorescence stems of plants with the weak phenotype grown with dexamethasone RNAi expression, the cells in files were shorter and the stomata were also in clusters (Figure 8C).

the central root (left) and close to the surface layer (right) show that all cell files are distorted in roots grown for 15 d with dexamethasone-induced RNAi expression. FM1-43 and propidium iodide staining are as in **(B)**. Bars = 10 μm.
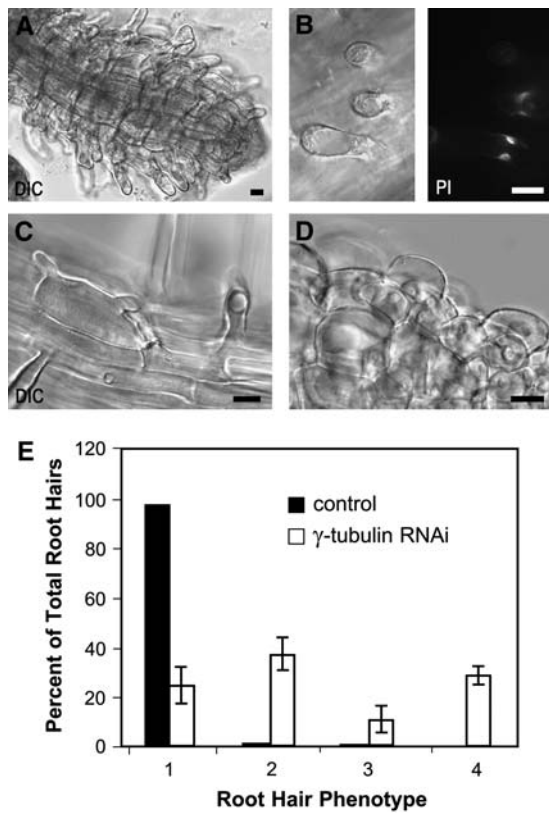
Figure 6. Ectopic Root Hair Formation and Loss of Polar Root Hair Growth in γ-Tubulin RNAi Plants.

(A) Ectopic root hairs formed along the entire root length in a γ-tubulin RNAi plant 8 d after dexamethasone induction. Bar = 10 μm.

(B) Two nuclei (right) stacked beneath an extremely large vacuole (left) in a short and wide root hair 10 d after dexamethasone induction. Bar = 10 μm.

(C) Two or more growth axes emerged from one root hair bulge 10 d after dexamethasone induction. Bar = 10 μm.

(D) Root hair bulges with failure of tip growth 12 d after dexamethasone induction. Bar = 10 μm.

(E) Percentage of root hair phenotypes in the control plants transformed with the empty cassette grown on dexamethasone and in dexamethasone-inducible RNAi plants. Bars 1, root hairs of wild-type phenotype; bars 2, short wide root hairs, as shown in **(B)**; bars 3, root hairs with two or more growth axes from one root hair bulge, as shown in **(C)**; bars 4, root hair bulges with failure of the transition to tip growth, as shown in **(D)**. Values shown represent means of the percentage counted for 10 plants; *n* = 1000. Error bars represent SD. Similar results were obtained with the ethanol-inducible RNAi lines.

Stomata clustering indicated that a slight reduction of γ-tubulin increases the number of guard mother cells produced, thus having an effect on stomata production but not on differentiation. However, stomata were not only found in clusters but also showed cytokinetic defects when γ-tubulin levels were severely reduced. A strong effect of RNAi on stomatal patterning and guard cell division is shown for plants in the mild phenotype category grown for 15 d with dexamethasone (Figure 8D) or ethanol (Figures 8E and 8F) induction. The stomata units were

defined as one or more guard cells in contact with each other, as used to characterize *too many mouths* (*tmm*) mutants with clustered stomata (Yang and Sack, 1995). We counted the number of stomata per stomata unit. It was found that in RNAi plants, ~40% of the stomata units contain more than one stoma and that ~45% of single and/or clustered stomata displayed the cytokinetic defect (Figure 8G). The stomata clusters were different in size, and a range of cytokinetic defects were present, including partial or missing ventral cell walls, unpaired stomata positioned side by side (Figures 8D and 8E), and lack of pores or pores plugged with callose deposits revealed by aniline blue staining (Figure 8F). To our knowledge, the effects of RNAi on stomata clustering and cytokinetic defects have not previously been observed in control uninduced transformants or in plants transformed with empty vectors and treated with dexamethasone or ethanol (Figure 8G). The stomata phenotypes were very similar in both the dexamethasone- and ethanol-inducible RNAi expression systems.

DISCUSSION

γ-Tubulin Is Required for Acentrosomal MT Nucleation

γ-Tubulin is primarily considered a universal minus end MT nucleator. This dogma is based on experiments with cells that have well-defined MTOCs. However, there is little evidence for such a role in cells that lack discrete sites for MT nucleation, including acentrosomal plant cells. Immunolocalization studies on various plant species and cell types showed that besides labeling the nuclear envelope and patchy pattern labeling in
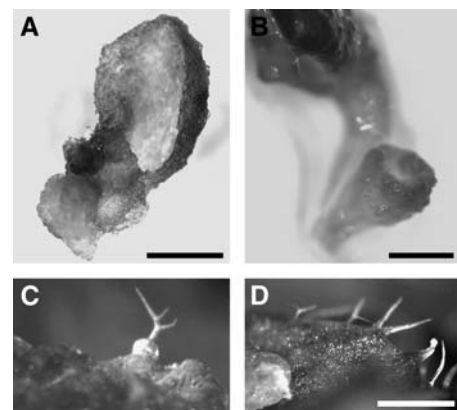
Figure 7. Leaf Phenotypes of RNAi Plants.

(A) Thick, curled leaves of plants with the mild phenotype, as shown in Figure 1C, grown for 15 d with RNAi induction. Leaves have roughened surfaces.
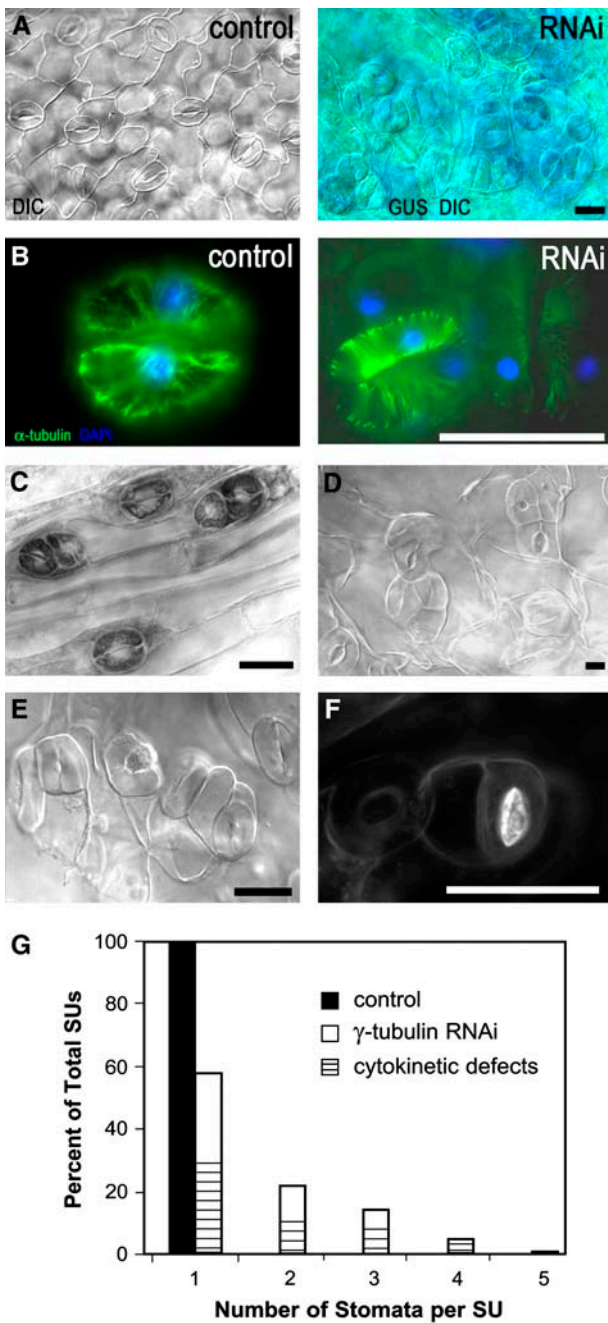
(B) The youngest leaves developed with reduced γ-tubulin levels have club-shaped blades.

(C) Trichomes with extremely swollen bases that appear with high frequency.

(D) Unbranched trichomes with bulged tips developed on leaves later upon RNAi induction, and the youngest malformed leaves were hairless **(B)**. Bars = 250 μm.

Figure 8. Stomatal Patterning and Differentiation Are Altered in RNAi Plants.

(A) Leaf epidermis of a control plant (left) and an RNAi plant of the weak phenotype grown in soil with dexamethasone induction for 21 d (right). Stomata are in clusters of two to four. Bar = 25 μm.
(B) Immunolocalization analysis of α-tubulin showing the presence of MTs in the control stomata (left) and in the stomata cluster from the γ-tubulin RNAi plant shown in **(A)** (right). Bar = 25 μm.
(C) Clustered stomata also appeared on inflorescence stems that developed with induced RNAi. Bar = 25 μm.
(D) and **(E)** Stomata were clustered and cytokinetic defects appeared in mild phenotype plants with more severe depletion of γ-tubulin (as shown

cytoplasm and with undefined membrane structures, the strongest signal for γ-tubulin is associated with all microtubular arrays (Liu et al., 1993, 1994; Dibbayawan et al., 2001; Drykova et al., 2003). This type of localization is inconsistent for a protein putatively involved in minus end–directed MT nucleation; thus, γ-tubulin was not considered a good marker for nucleation sites in plant cells (Lloyd and Chan, 2004). Previously, we demonstrated that cellular fractions enriched in γ-tubulin promote MT formation, either by stabilization or through nucleation (Drykova et al., 2003). Here, we provide several lines of evidence for γ-tubulin–dependent MT nucleation from dispersed sites in plants. (1) MTs were absent in cells with RNAi depletion of γ-tubulin; as a result, there are some shared phenotypes between cells depleted for γ-tubulin and cells treated with drugs that induce MT depolymerization, such as the loss of anisotropic growth, vacuolization, and fragility of the cell walls. (2) Recovery of MTs after drug depolymerization was impaired in RNAi plants by reduced γ-tubulin levels. (3) Nearly complete immunodepletion of γ-tubulin from extracts prevented taxol-promoted MT polymerization in vitro.

In fungi and in animal cells, well-characterized γ-tubulin complexes become part of the spindle pole bodies or the centrosomes, where they provide templates for minus end MT nucleation (Geissler et al., 1998; Oegema et al., 1999). A search for such complexes in acentrosomal plant cells was unsuccessful, although the plant homologue of Spc98p, a protein that interacts with γ-tubulin in protein complexes in a broad range of eukaryotes, was described in plants (Erhardt et al., 2002). In plant cells, cytoplasmic γ-tubulin ring complexes have not yet been identified; rather, we found the presence of heterogeneous protein complexes of plant γ-tubulin in cytoplasm in association with membranes and MTs (Drykova et al., 2003). Using biochemical fractionation and immunofluorescence, we show that RNAi induction equally depleted γ-tubulin from all known locations, including the microsomal and microtubular fractions, and severe depletion prevented the formation of MTs. Furthermore, we found that the regrowth of MTs from the perinuclear membrane–rich region after drug depolymerization was delayed in cells with reduced γ-tubulin levels. Extracentrosomal templates with γ-tubulin are known to exist and nucleate MTs in other organisms. MT nucleation from membrane-associated γ-tubulin was observed for myotubes (Tassin et al., 1985), for nuclear membrane fragments in *Drosophila* spermatocytes (Rebollo et al., 2004), for the perinuclear region of *Drosophila* oocytes (Januschke et al., 2006), and for Golgi membranes in mammalian cells (Chabin-Brion et al., 2001). Self-organization of γ-tubulin–containing material, which relies on the continuous association of nucleation sites with MTs, was described recently in *S. pombe*

in Figure 1C) upon dexamethasone **(D)** or ethanol **(E)** RNAi induction for 15 d. Bar = 25 μm.
(F) Callose deposits in a stomata with aberrant division after RNAi induction for 15 d. Bar = 25 μm.
(G) Frequencies of stomata units (SUs) with clustered stomata and with or without the cytokinetic defect in ethanol- and dexamethasone-induced RNAi-expressing plants with the defects shown in **(D)** to **(F)**. n = 500 for the control and 500 for RNAi plants.

(Zheng et al., 2006). Dispersed γ-tubulin–containing nucleation sites in plants might be dynamically reorganized in a similar self-organizing process to create membrane-bound and MT-bound MTOCs that enable the nucleation, bundling, and intracellular positioning of MT arrays. Understanding the molecular mechanisms of MT nucleation from those dispersed sites will require further studies.

γ-Tubulin Is a Component of Cortical Templates That Guide the MT Network

In plants, highly dynamic cortical MTs are arranged into regular arrays and rapidly adopt the directionality of anisotropic growth in response to hormones, environmental cues, and differentiation. Here, we show that the parallel cortical MTs of differentiating *Arabidopsis* cells were sensitive to the reduction of γ-tubulin levels by RNAi; γ-tubulin rapidly disappeared from its locations on the plasma membrane and from cortical MTs that became bundled and randomized. Recently, a model was proposed for the self-organization of cortical MTs. It was shown that intermicrotubule interactions among newly formed short MTs are sufficient to facilitate the organization of plant cortical MTs into a parallel configuration (Dixit and Cyr, 2004). Reduction of cortical MT-bound γ-tubulin, which acts as a nucleator, might disturb the balanced rate of tubulin polymerization needed to maintain minimum cortical MT length, which is a prerequisite for self-organization and for guiding MTs into parallel networks. Drugs that reduce the rate of MT polymerization also shorten cortical MTs and disturb their transverse orientation (Thitamadee et al., 2002). Randomized short cortical MTs are also present in *Arabidopsis* mutants for the plant homologue of katanin, a protein that severs MTs from nucleation sites (Burk and Ye, 2002). Thus, our RNAi data suggest that both γ-tubulin–mediated nucleation and the severing of MTs from existing nucleation sites are important to generate new MTs and enable their self-organization into transverse arrays. Recently, the nucleation of MTs from preexisting cortical MTs was shown to require the binding of cytoplasmic γ-tubulin to cortical MTs in tobacco cells (Murata et al., 2005). These findings are fully consistent with our observation of the effect of γ-tubulin RNAi on cortical MTs. Linear MT arrays are not plant cell–specific but are also formed in polarized animal cells, such as neurones, epithelial cells, and myotubes (Dammermann et al., 2003). In *S. pombe*, nucleation from γ-tubulin complexes along the length of existing MTs was shown to drive the formation of bipolar MT bundles (Janson et al., 2005). Similar mechanisms might then optimize the generation and spacing of multiple bipolar MT bundles in fungi, animal cells, and plants.

γ-Tubulin Is Important for Polar Cell Expansion

The radial expansion of roots was not unexpected in γ-tubulin RNAi plants, in which the function of the MT cytoskeleton was impaired by reducing the number of nucleation sites and by randomization of cortical MTs. Randomization or loss of cortical MTs is known to disrupt anisotropic growth (Baskin et al., 2004). However, the mechanisms by which MTs control cell wall formation and hence plant cell shape and polarity are not fully understood. The glycosylphosphatidylinositol proteins were recently suggested to be effectors of MT function in controlling mechanical properties of cellulose microfibrils and thus in establishing and maintaining axial growth (Wasteneys and Fujita, 2005).

Randomization of cortical MTs upon induction of γ-tubulin RNAi expression may be a prerequisite for ectopic root hair formation, as it was also found in plants treated with anti-MT drugs (Sugimoto et al., 2003) and in the katanin mutants (Webb et al., 2002). Once cell fate is specified, the process of root hair formation appears to be less affected by MT-disrupting drugs (Bibikova et al., 1999) and the polar growth is thought to be more actin-driven. The γ-tubulin RNAi root hair phenotypes with defective transition from root hair initiation to tip growth and with loss of the polar growth axis are thus surprising. Our findings either indicate a novel role for MTs in root hair polar tip growth or reveal an unknown role for γ-tubulin in polar tip growth.

γ-Tubulin was always thought to be a universal minus end MT nucleator. However, recent data on *S. pombe* showed that γ-tubulin might affect various properties of MTs, including plus end dynamics (Zimmerman and Chang, 2005). There is evidence to suggest that plants possess the core machinery similar to that required for the determination of polarity in *S. pombe* and for forward motility in animal cells, in which actin closely interacts with protein complexes of the leading plus ends of MTs (Mathur, 2005). Hence, γ-tubulin might play a role in processes that link plus end MT dynamics and polarity determination processes in plants.

γ-Tubulin Is Essential for the Coordination of Late Mitotic Events

RNAi-reduced levels of centrosomal γ-tubulin were found to lead to monopolar or multipolar spindle formation in *C. elegans* and to aberrant spindle formation in the vicinity of chromatin in *Drosophila* (Hannak et al., 2002; Raynaud-Messina et al., 2004). We found that the bipolarity of plant mitosis is less sensitive to the RNAi reduction of spindle-localized γ-tubulin. Only severe depletion of γ-tubulin resulted in the collapse of spindles, and only remnants of MTs in these cells were found in the vicinity of chromatin. Although mitosis was little affected by the reduced levels of γ-tubulin, cytokinesis frequently became defective, showing mainly misorientation of the cell division site and temporal uncoupling of the cytokinetic events. A lack of coordination of mitotic events was also found in conditional γ-tubulin mutants in *Aspergillus* and in *S. pombe*: mitotic MTs were formed in spite of the impaired γ-tubulin function, but cytokinesis became abnormal (Paluh et al., 2000; Hendrickson et al., 2001). The position of the mitotic spindle provides positional clues for cell plate formation in *S. pombe* (Oliferenko and Balasubramanian, 2002). Dispersed γ-tubulin–containing MTOCs are critical for the correct anchorage of the cytokinetic actin ring and the proper coordination of mitosis with cytokinesis in *S. pombe* (Venkatram et al., 2005). Our data suggest that a similar mechanism might also operate in plant cells with dispersed MTOCs. γ-Tubulin interconnects membrane organization with positional clues such as centrosomes during cell cycle progression in mammalian cells (Rios et al., 2004). The regulatory mechanisms of the dynamic

relocation of γ-tubulin during mitosis and cytokinesis in acentrosomal plants and their impact on progression through cell division remain to be elucidated.

Cytokinetic defects were observed in many different cell types after RNAi depletion of γ-tubulin in plants, including stomata. Stomatal complexes as terminal products of a cell lineage are generated by a strictly controlled series of asymmetric and symmetric divisions (Geisler et al., 2003). We found that clustering of stomata occurred even in plants that showed only a slight reduction in γ-tubulin levels and had only subtle phenotypic changes and no apparent MT reorganization. Stomatal clustering was similar to the phenotype of the *Arabidopsis tmm* mutants, in which the plane and the frequency of division are disrupted as a result of the absence of a presumptive negative regulator of asymmetric cell division (Yang and Sack, 1995). Thus, in *tmm* mutants, the asymmetric divisions are randomized and divisions occur in cells located next to two stomata or in precursor cells that normally would never divide. A null mutation in YODA, an *Arabidopsis* mitogen-activated kinase kinase kinase, affected the asymmetric division of precursor cells and led to excess stomata in clusters (Bergmann et al., 2004). It is not clear yet how the perception of spatial information from the precursor cell is transduced to control cell cycle progression and specify correctly the plane of asymmetric division in stomatal patterning. Our experiments show that γ-tubulin plays an important role in executing asymmetric cell division during stomatal patterning.

As the reduction of γ-tubulin got progressively stronger, the stomata were not only clustered but also exhibited defective guard cell divisions, such as absent or incomplete pores, partial or missing ventral cell walls, and unpaired stomata. In *flp* mutants, pore thickening does not develop and guard cells divide again, forming clusters of unpaired guard cells; *flp* acts later in the stomatal patterning pathway than does *tmm* (Yang and Sack, 1995). In our experiments, first stomatal patterning and then cytokinesis of guard cells were disrupted, with increasing reductions in γ-tubulin levels, suggesting that γ-tubulin is required in both processes but at different levels. We do not yet know whether the cell specification during stomata development requires γ-tubulin function that relies on the regulation of MT properties or whether the patterning, cell cycle, and cell polarity defects reflect as yet undiscovered roles for γ-tubulin that are independent of MTs.

In summary, we have shown that γ-tubulin is essential for MT nucleation from dispersed sites in plant cells. γ-Tubulin, as a component of cortical nucleation templates, guides cortical MTs and is required for their dynamic organization. Gradual and stepwise diminution of γ-tubulin allowed us to reveal roles for MTs in plant development. Our data also indicate that in addition to its nucleation role, other still unknown functions for γ-tubulin exist in the regulation of MT properties, in the coordination of late mitotic events, and in cell specification.

METHODS

Constructs and Plant Transformation

The γ-tubulin RNAi vector was constructed by generating an inverted hairpin loop. A 722-bp fragment corresponding to nucleotides 700 to 1425 of the *Arabidopsis thaliana* TubG1 3′ terminal sequence was amplified using two primers: AtTubG1/2-F (5′-TTGCTCGAGGATCCAC-TGTGATGTCTGCTAGCAC-3′) and AtTubG1/2-R (5′-TTCGAATTCATC-GATCAACTCCTGAAGCATTGCCTTCC-3′). The PCR fragment was cloned directly into pGEM-T vector (Promega) and confirmed by sequencing. After digestion with *Bam*HI-*Cla*I and *Xho*I-*Eco*RI, respectively, the resulting fragments (corresponding to sense and antisense arms) were cloned into pART69 to generate the RNAi intermediate construct.

For glucocorticoid-inducible expression, a *Bam*HI-*Bam*HI fragment containing both arms was isolated and subcloned into binary vector pHGUSK (Craft et al., 2005), generating an inducible RNAi reporter construct, pHGUSK:TubG1-RNAi. For ethanol-inducible expression, a *Bam*HI-*Bam*HI fragment containing both arms was isolated and subcloned into binary vector pGreenAlcA (Deveaux et al., 2003).

The glucocorticoid-inducible pHGUSK:TubG1-RNAi vector was introduced into *Agrobacterium tumefaciens* strain GV3101. *Arabidopsis* (ecotype Columbia) activator line 4C-S5 (Craft et al., 2005) was transformed by the floral dip method. Seeds collected from transformed plants were plated on Murashige and Skoog (MS) agar plates containing hygromycin (15 mg/L) for selection. To confirm the presence of the construct, PCR with gene-specific primers was performed on genomic DNA. Primary transformants containing the pGreenAlcA:TubG1-RNAi were selected by repeated spraying of seedlings with a 250-mg/mL solution of the herbicide Chalenge (Agro Evo) until the growth differences were clear. Seeds collected from transformed plants were plated onto MS growth medium with 25 mg/L phosphoinotricine for selection of T2 plants. Seven-day-old seedlings were transferred to MS medium with or without ethanol induction.

Wild-type *Arabidopsis* and activator plants for either glucocorticoid- or ethanol-inducible expression transformed with an empty vector were used as controls.

Plant Material

Arabidopsis seeds of control and transformed plants were surface-sterilized by soaking in 10% bleach plus 0.05% Triton X-100 for 15 min followed by three washes in sterile water. Subsequently, the seeds were plated on 1% (w/v) agar plates containing MS medium (Duchefa), 0.25 mM MES, and 1% saccharose. After 3 d of stratification at 4°C, seedlings were grown on horizontally or vertically oriented plates. Plants were grown in pots at 20°C under short-day conditions (8 h of light/16 h of dark) for 3 weeks and then under long-day conditions (16 h of light/8 h of dark).

Induction of γ-Tubulin RNAi Expression

Dexamethasone (Sigma-Aldrich; 60 mM stock solution in DMSO) was supplemented in the culture medium at final concentrations of 10 to 30 μM. Seedlings were germinated and grown on the induction medium for various periods or transferred for induction from MS medium at different time points. For RNAi induction in liquid medium supplemented with 10 to 20 μM dexamethasone, 3- to 5-d-old seedlings were transferred from solid medium into the flasks or a multiwell culture chamber and shaken (~90 rpm) at 23°C. Plants grown in soil were watered once per week with 25 mL of 20 μM dexamethasone; 0.02% Silwet was also applied locally to the leaves or flowers. Mock treatment with DMSO was used as a control in every experiment. Ethanol treatments for induction of the RNAi transgene were performed according to Ketelaar et al. (2004).

GUS activity was determined and histochemically localized for analysis of GUS reporter activity according to Jefferson et al. (1987). Histochemically analyzed tissues were observed directly or cleared in Hoyer's medium at least overnight at room temperature as described previously (Liu and Meinke, 1998).

Preparation of Cell Extracts, Electrophoresis, and Immunoblotting

Seedlings were ground in liquid nitrogen, thawed in 1 to 2 volumes of extraction buffer supplemented with protease and phosphatase inhibitor cocktail (Drykova et al., 2003), and centrifuged at 10,000g for 10 min at 4°C. To obtain microsomal pellets, extracts were further centrifuged at 100,000g for 1 h at 4°C. Proteins separated by SDS-PAGE were transferred onto nitrocellulose membranes by wet electroblotting (Amersham Biosciences). Immunoreactive bands were visualized using the enhanced chemiluminescence detection system.

Immunodepletion

Extracts of 3-d-old *Arabidopsis* cell culture were prepared by grinding the cells (4 g wet weight) in liquid nitrogen and suspending the powder in 5 mL of buffer BrB80 (80 mM K-Pipes, 1 mM MgCl$_2$, and 1 mM EGTA, pH 6.9) supplemented with 10% glycerol and 1 mM GTP plus protease and phosphatase inhibitor cocktail. Centrifugation of homogenates at 10,000g for 10 min was followed by a 30-min centrifugation at 70,000g. The final supernatant (S70; 0.5 mL, 3.5 mg protein/mL) was incubated for 2 h at room temperature with 100 μL of the protein A–purified rabbit anti-γ-tubulin antibody AthTU (Drykova et al., 2003) and 100 μL of protein A–Sepharose beads (Amersham Biosciences). The beads were pelleted, and immunodepletion was repeated with the supernatant supplemented with 50 μL of AthTU antibody and 50 μL of protein A beads with 4-h incubations at 4°C. The immunodepleted supernatants were tested for residual γ-tubulin using protein gel immunoblot–enhanced chemiluminescence with TU-31 mouse monoclonal anti-γ-tubulin antibody (Drykova et al., 2003). As a control mock depletion, preimmune serum was used instead of antibody. The untreated S70 extracts served as a positive control. The immunodepleted, the mock-depleted, and the control extract were used as input extracts for the MT polymerization assays.

MT Polymerization Assay

MT spin-down experiments were performed as described previously (Weingartner et al., 2001; Drykova et al., 2003). MTs were polymerized from the input extracts obtained in immunodepletion experiments that were supplemented with GTP to 1 mM and with taxol (Sigma-Aldrich) to 20 μM. Pelleted MTs were resuspended in SDS sample buffer and loaded together with supernatants for electrophoresis and protein gel blotting.

Cover Slip Assays for Plant MT Polymerization

The cover slip nucleation assay was performed as described (Drykova et al., 2003) with the immunodepleted, the mock-depleted, and the control *Arabidopsis* cell extracts. After MT polymerization, cover slips were mounted on the slides in Tris-buffered saline and observed microscopically using DIC optics or processed for immunofluorescent labeling to visualize MTs (Drykova et al., 2003). Anti-α-tubulin antibody and fluorescein isothiocyanate (FITC)– and Cy3-conjugated secondary antibodies were used as described below for immunofluorescence.

Immunofluorescence

Arabidopsis seedlings, dissected parts of seedlings, or cultured cells of *Arabidopsis* were fixed for 1 h using 3.7% formaldehyde made fresh from paraformaldehyde and processed for immunofluorescence (Binarova et al., 1993). For whole-mount immunolabeling, the seedlings were treated with enzyme mixture (0.5% cellulase, 1% driselase, and 0.025% pectolyase), and incubation with primary and secondary antibodies was prolonged to 2 h at room temperature or overnight at 4°C. Primary antibodies (anti-α-tubulin monoclonal antibody DM1A [Sigma-Aldrich] at a dilution of 1:500, monoclonal anti-γ-tubulin TU-31 as an undiluted supernatant, and affinity-purified rabbit polyclonal antibody AthTU at a dilution of 1:1000) (Drykova et al., 2003) were used with anti-mouse FITC-conjugated or anti-rabbit Cy3-conjugated secondary antibodies (Sigma-Aldrich). After DAPI staining of DNA, the samples were mounted onto slides.

FM1-43 Fluorescent Dye Staining of Plasma Membrane, Callose Staining with Aniline Blue, and Propidium Iodide Staining of Nuclei

Staining of the membranes with FM1-43 (Molecular Probes) was performed as described (Volker et al., 2001). Nuclei were labeled with 0.1 mg/mL propidium iodide (Sigma-Aldrich) for 10 min. Callose was detected by adding 0.1 mM aniline blue (Sigma-Aldrich) to the culture medium for 2 h at room temperature.

For APM treatment, 7-d-old seedlings were transferred to liquid or MS solid medium supplemented with the MT-depolymerizing drug APM at final concentrations of 0.1 and 5 μM and treated for 1 to 7 d.

Microscopy and Confocal Microscopy

Microscopy was performed on an Olympus universal microscope equipped with epifluorescence optics (model Provis AX70 optical microscope equipped with a 100/1.4 oil-immersion objective) as well as a Sensi Cam cooled charge-coupled device camera (Kelheim) and using Micro Image Olympus optical software. To avoid filter crosstalk, fluorescence was detected using HQ 480/40 exciter and HQ 510/560 emitter filter cubes for FITC and HQ 545/30 exciter and HQ 610/75 emitter filter cubes for Cy3 (both AHF Analysen Technique). Filters for DIC were used for the observation of MTs polymerized in cover slip nucleation assays. Confocal images were taken using a Leica TCS/SP laser-scanning confocal microscope with or without the two-photon mode. Laser scanning was performed using the sequential multitrack mode to avoid bleed through. Excitation and emission wavelengths were 488 nm and 505 to 532 nm for FITC and 543 nm and 566 to 600 nm for Cy3. Seedlings were mounted on fresh medium. Excitation and emission wavelengths were 488 nm and 500 to 530 nm plus 580 to 630 nm for FM1-43, 530 and 615 nm for propidium iodide, and 405 nm and 420 to 490 nm for aniline blue. Green fluorescent protein was excited using 488 nm and imaged using emission filter 500/550 nm. Images were contrast-enhanced using image-processing software (Photoshop; Adobe Systems).

Accession Number

Sequence data for *Arabidopsis* TubG1 can be found in the GenBank data library under accession number U02069.

Supplemental Data

The following materials are available in the online version of this article.

   Supplemental Figure 1. Strength of the Phenotype and Strength of GUS Staining of Transformants Expressing the Dexamethasone-Inducible γ-Tubulin RNAi Construct.

   Supplemental Figure 2. Lack of MT Polymerization from Extracts Immunodepleted for γ-Tubulin Observed on Cover Slips in in Vitro Polymerization Assays.

   Supplemental Figure 3. MTs in Root Hairs of Control and RNAi Plants.

REFERENCES

Baskin, T.I., Beemster, G.T., Judy-March, J.E., and Marga, F. (2004). Disorganization of cortical microtubules stimulates tangential expansion and reduces the uniformity of cellulose microfibril alignment among cells in the root of Arabidopsis. Plant Physiol. **135,** 2279–2290.

Bergmann, D.C., Lukowitz, W., and Somerville, C.R. (2004). Stomata development and pattern controlled by a MAPKK kinase. Science **304,** 1461–1462.

Bibikova, T.N., Blancaflor, E.B., and Gilroy, S. (1999). Microtubules regulate tip growth and orientation in root hairs of *Arabidopsis thaliana.* Plant J. **17,** 657–665.

Binarova, P., Cenklova, V., Hause, B., Kubatova, E., Lysak, M., Dolezel, J., Bogre, L., and Draber, P. (2000). Nuclear gamma-tubulin during acentriolar plant mitosis. Plant Cell **12,** 433–442.

Binarova, P., Cihalikova, J., and Dolezel, J. (1993). Localization of MPM-2 recognized phosphoproteins and tubulin during cell cycle progression in synchronized *Vicia faba* root meristem cells. Cell Biol. Int. **17,** 847–856.

Brown, R.C., Lemmon, B.E., and Horio, T. (2004). Gamma-tubulin localization changes from discrete polar organizers to anastral spindles and phragmoplasts in mitosis of *Marchantia polymorpha* L. Protoplasma **224,** 187–193.

Burk, D.H., and Ye, Z.H. (2002). Alteration of oriented deposition of cellulose microfibrils by mutation of a katanin-like microtubule-severing protein. Plant Cell **14,** 2145–2160.

Chabin-Brion, K., Marceiller, J., Perez, F., Settegrana, C., Drechou, A., Durand, G., and Pous, C. (2001). The Golgi complex is a microtubule-organizing organelle. Mol. Biol. Cell **12,** 2047–2060.

Craft, J., Samalova, M., Baroux, C., Townley, H., Martinez, A., Jepson, I., Tsiantis, M., and Moore, I. (2005). New pOp/LhG4 vectors for stringent glucocorticoid-dependent transgene expression in Arabidopsis. Plant J. **41,** 899–918.

Dammermann, A., Desai, A., and Oegema, K. (2003). The minus end in sight. Curr. Biol. **13,** R614–R624.

Deveaux, Y., Peaucelle, A., Roberts, G.R., Coen, E., Simon, R., Mizukami, Y., Traas, J., Murray, J.A., Doonan, J.H., and Laufs, P. (2003). The ethanol switch: a tool for tissue-specific gene induction during plant development. Plant J. **36,** 918–930.

Dibbayawan, T.P., Harper, J.D., and Marc, J. (2001). A gamma-tubulin antibody against a plant peptide sequence localises to cell division-specific microtubule arrays and organelles in plants. Micron **32,** 671–678.

Dixit, R., and Cyr, R. (2004). Encounters between dynamic cortical microtubules promote ordering of the cortical array through angle-dependent modifications of microtubule behavior. Plant Cell **16,** 3274–3284.

Drykova, D., Cenklova, V., Sulimenko, V., Volc, J., Draber, P., and Binarova, P. (2003). Plant gamma-tubulin interacts with alphabeta-tubulin dimers and forms membrane-associated complexes. Plant Cell **15,** 465–480.

Erhardt, M., Stoppin-Mellet, V., Campagne, S., Canaday, J., Mutterer, J., Fabian, T., Sauter, M., Muller, T., Peter, C., Lambert, A.M., and Schmit, A.C. (2002). The plant Spc98p homologue colocalizes with gamma-tubulin at microtubule nucleation sites and is required for microtubule nucleation. J. Cell Sci. **115,** 2423–2431.

Geisler, M.J., Deppong, D.O., Nadeau, J.A., and Sack, F.D. (2003). Stomatal neighbor cell polarity and division in Arabidopsis. Planta **216,** 571–579.

Geissler, S., Siegers, K., and Schiebel, E. (1998). A novel protein complex promoting formation of functional alpha- and gamma-tubulin. EMBO J. **17,** 952–966.

Hannak, E., Oegema, K., Kirkham, M., Gonczy, P., Habermann, B., and Hyman, A.A. (2002). The kinetically dominant assembly pathway for centrosomal asters in *Caenorhabditis elegans* is gamma-tubulin dependent. J. Cell Biol. **157,** 591–602.

Hendrickson, T.W., Yao, J., Bhadury, S., Corbett, A.H., and Joshi, H.C. (2001). Conditional mutations in gamma-tubulin reveal its involvement in chromosome segregation and cytokinesis. Mol. Biol. Cell **12,** 2469–2481.

Horio, T., and Oakley, B.R. (2003). Expression of Arabidopsis gamma-tubulin in fission yeast reveals conserved and novel functions of gamma-tubulin. Plant Physiol. **133,** 1926–1934.

Janson, M.E., Setty, T.G., Paoletti, A., and Tran, P.T. (2005). Efficient formation of bipolar microtubule bundles requires microtubule-bound gamma-tubulin complexes. J. Cell Biol. **169,** 297–308.

Januschke, J., Gervais, L., Gillet, L., Keryer, G., Bornens, M., and Guichet, A. (2006). The centrosome-nucleus complex and microtubule organization in the Drosophila oocyte. Development **133,** 129–139.

Jefferson, R.A., Kavanagh, T.A., and Bevan, M.W. (1987). GUS fusions: Beta-glucuronidase as a sensitive and versatile gene fusion marker in higher plants. EMBO J. **6,** 3901–3907.

Ketelaar, T., Allwood, E.G., Anthony, R., Voigt, B., Menzel, D., and Hussey, P.J. (2004). The actin-interacting protein AIP1 is essential for actin organization and plant development. Curr. Biol. **14,** 145–149.

Lesca, C., Germanier, M., Raynaud-Messina, B., Pichereaux, C., Etievant, C., Emond, S., Burlet-Schiltz, O., Monsarrat, B., Wright, M., and Defais, M. (2005). DNA damage induce gamma-tubulin-RAD51 nuclear complexes in mammalian cells. Oncogene **24,** 5165–5172.

Liu, B., Joshi, H.C., Wilson, T.J., Silflow, C.D., Palevitz, B.A., and Snustad, D.P. (1994). Gamma-tubulin in Arabidopsis: Gene sequence, immunoblot, and immunofluorescence studies. Plant Cell **6,** 303–314.

Liu, B., Marc, J., Joshi, H.C., and Palevitz, B.A. (1993). A gamma-tubulin-related protein associated with the microtubule arrays of higher plants in a cell cycle-dependent manner. J. Cell Sci. **104,** 1217–1228.

Liu, C.M., and Meinke, D.W. (1998). The titan mutants of Arabidopsis are disrupted in mitosis and cell cycle control during seed development. Plant J. **16,** 21–31.

Lloyd, C., and Chan, J. (2004). Microtubules and the shape of plants to come. Nat. Rev. Mol. Cell Biol. **5,** 13–22.

Mathur, J. (2005). Conservation of boundary extension mechanisms between plants and animals. J. Cell Biol. **168,** 679–682.

Moritz, M., Braunfeld, M.B., Fung, J.C., Sedat, J.W., Alberts, B.M., and Agard, D.A. (1995). Three-dimensional structural characterization of centrosomes from early Drosophila embryos. J. Cell Biol. **130,** 1149–1159.

Murata, T., Sonobe, S., Baskin, T.I., Hyodo, S., Hasezawa, S., Nagata, T., Horio, T., and Hasebe, M. (2005). Microtubule-dependent

microtubule nucleation based on recruitment of gamma-tubulin in higher plants. Nat. Cell Biol. **7,** 961–968.

Oegema, K., Wiese, C., Martin, O.C., Milligan, R.A., Iwamatsu, A., Mitchison, T.J., and Zheng, Y. (1999). Characterization of two related Drosophila gamma-tubulin complexes that differ in their ability to nucleate microtubules. J. Cell Biol. **144,** 721–733.

Oliferenko, S., and Balasubramanian, M.K. (2002). Astral microtubules monitor metaphase spindle alignment in fission yeast. Nat. Cell Biol. **4,** 816–820.

Paluh, J.L., Nogales, E., Oakley, B.R., McDonald, K., Pidoux, A.L., and Cande, W.Z. (2000). A mutation in gamma-tubulin alters microtubule dynamics and organization and is synthetically lethal with the kinesin-like protein pkl1p. Mol. Biol. Cell **11,** 1225–1239.

Prigozhina, N.L., Oakley, C.E., Lewis, A.M., Nayak, T., Osmani, S.A., and Oakley, B.R. (2004). Gamma-tubulin plays an essential role in the coordination of mitotic events. Mol. Biol. Cell **15,** 1374–1386.

Raynaud-Messina, B., Mazzolini, L., Moisand, A., Cirinesi, A.M., and Wright, M. (2004). Elongation of centriolar microtubule triplets contributes to the formation of the mitotic spindle in {gamma}-tubulin-depleted cells. J. Cell Sci. **117,** 5497–5507.

Rebollo, E., Llamazares, S., Reina, J., and Gonzalez, C. (2004). Contribution of noncentrosomal microtubules to spindle assembly in Drosophila spermatocytes. PLoS Biol. **2,** E8.

Reilein, A., and Nelson, W.J. (2005). APC is a component of an organizing template for cortical microtubule networks. Nat. Cell Biol. **7,** 463–473.

Rios, R.M., Sanchis, A., Tassin, A.M., Fedriani, C., and Bornens, M. (2004). GMAP-210 recruits gamma-tubulin complexes to cis-Golgi membranes and is required for Golgi ribbon formation. Cell **118,** 323–335.

Schmit, A.C. (2002). Acentrosomal microtubule nucleation in higher plants. Int. Rev. Cytol. **220,** 257–289.

Shaw, S.L., Kamyar, R., and Ehrhardt, D.W. (2003). Sustained microtubule treadmilling in Arabidopsis cortical arrays. Science **300,** 1715–1718.

Strome, S., Powers, J., Dunn, M., Reese, K., Malone, C.J., White, J., Seydoux, G., and Saxton, W. (2001). Spindle dynamics and the role of gamma-tubulin in early *Caenorhabditis elegans* embryos. Mol. Biol. Cell **12,** 1751–1764.

Sugimoto, K., Himmelspach, R., Williamson, R.E., and Wasteneys, G.O. (2003). Mutation or drug-dependent microtubule disruption causes radial swelling without altering parallel cellulose microfibril deposition in Arabidopsis root cells. Plant Cell **15,** 1414–1429.

Tassin, A.M., Maro, B., and Bornens, M. (1985). Fate of microtubule-organizing centers during myogenesis in vitro. J. Cell Biol. **100,** 35–46.

Thitamadee, S., Tuchihara, K., and Hashimoto, T. (2002). Microtubule basis for left-handed helical growth in Arabidopsis. Nature **417,** 193–196.

Vaughn, K.C., and Harper, J.D. (1998). Microtubule-organizing centers and nucleating sites in land plants. Int. Rev. Cytol. **181,** 75–149.

Venkatram, S., Jennings, J.L., Link, A., and Gould, K.L. (2005). Mto2p, a novel fission yeast protein required for cytoplasmic microtubule organization and anchoring of the cytokinetic actin ring. Mol. Biol. Cell **16,** 3052–3063.

Volker, A., Stierhof, Y.D., and Jurgens, G. (2001). Cell cycle-independent expression of the Arabidopsis cytokinesis-specific syntaxin KNOLLE results in mistargeting to the plasma membrane and is not sufficient for cytokinesis. J. Cell Sci. **114,** 3001–3012.

Vorobjev, I., Malikov, V., and Rodionov, V. (2001). Self-organization of a radial microtubule array by dynein-dependent nucleation of microtubules. Proc. Natl. Acad. Sci. USA **98,** 10160–10165.

Wasteneys, G.O., and Fujita, M. (2006). Establishing and maintaining axial growth: Wall mechanical properties and the cytoskeleton. J. Plant Res. **119,** 5–10.

Webb, M., Jouannic, S., Foreman, J., Linstead, P., and Dolan, L. (2002). Cell specification in the *Arabidopsis* root epidermis requires the activity of ECTOPIC ROOT HAIR 3—a katanin-p60 protein. Development **129,** 123–131.

Weingartner, M., Binarova, P., Drykova, D., Schweighofer, A., David, J.P., Heberle-Bors, E., Doonan, J., and Bogre, L. (2001). Dynamic recruitment of Cdc2 to specific microtubule structures during mitosis. Plant Cell **13,** 1929–1943.

Yang, M., and Sack, F.D. (1995). The too many mouths and four lips mutations affect stomatal production in Arabidopsis. Plant Cell **7,** 2227–2239.

Zheng, L., Schwartz, C., Wee, L., and Oliferenko, S. (2006). The fission yeast TACC-related protein, Mia1p/Alp7p, is required for formation and maintenance of persistent microtubule-organizing centers at the nuclear envelope. Mol. Biol. Cell, in press.

Zimmerman, S., and Chang, F. (2005). Effects of {gamma}-tubulin complex proteins on microtubule nucleation and catastrophe in fission yeast. Mol. Biol. Cell **16,** 2719–2733.